


The effect of carbamazepine on bone structure and strength in control and osteogenesis imperfecta (*Col1a2*^{+/*p.G610C*}) mice

Martha Blank^{1,2} | Narelle E. McGregor¹ | Lynn Rowley³ | Louise H. W. Kung³ |
 Blessing Crimeen-Irwin¹ | Ingrid J. Poulton¹ | Emma C. Walker¹ | Jonathan H. Gooi⁴ |
 Shireen R. Lamandé^{3,5} | Natalie A. Sims^{1,2} | John F. Bateman^{3,5} 

¹Bone Cell Biology and Disease Unit, St. Vincent's Institute of Medical Research, Melbourne, Victoria, Australia

²Department of Medicine, The University of Melbourne, St. Vincent's Hospital, Melbourne, Victoria, Australia

³Musculoskeletal Research, Murdoch Children's Research Institute, Melbourne, Victoria, Australia

⁴Department of Biochemistry and Molecular Biology, Bio21 Molecular Science and Biotechnology Institute, University of Melbourne, Parkville, Victoria, Australia

⁵Department of Paediatrics, University of Melbourne, Melbourne, Victoria, Australia

Correspondence

John F. Bateman, Murdoch Children's Research Institute, Melbourne, Victoria 3052, Australia.
 Email: john.bateman@mcri.edu.au

Funding information

National Health and Medical Research Council, Grant/Award Number: GNT 1049863, GNT 1154819; Victorian Government's Operational Infrastructure Support Program; St. Vincent's Institute

Abstract

The inherited brittle bone disease osteogenesis imperfecta (OI) is commonly caused by *COL1A1* and *COL1A2* mutations that disrupt the collagen I triple helix. This causes intracellular endoplasmic reticulum (ER) retention of the misfolded collagen and can result in a pathological ER stress response. A therapeutic approach to reduce this toxic mutant load could be to stimulate mutant collagen degradation by manipulating autophagy and/or ER-associated degradation. Since carbamazepine (CBZ) both stimulates autophagy of misfolded collagen X and improves skeletal pathology in a metaphyseal chondrodysplasia model, we tested the effect of CBZ on bone structure and strength in 3-week-old male OI *Col1a2*^{+/*p.G610C*} and control mice. Treatment for 3 or 6 weeks with CBZ, at the dose effective in metaphyseal chondrodysplasia, provided no therapeutic benefit to *Col1a2*^{+/*p.G610C*} mouse bone structure, strength or composition, measured by micro-computed tomography, three point bending tests and Fourier-transform infrared microspectroscopy. In control mice, however, CBZ treatment for 6 weeks impaired femur growth and led to lower femoral cortical and trabecular bone mass. These data, showing the negative impact of CBZ treatment on the developing mouse bones, raise important issues which must be considered in any human clinical applications of CBZ in growing individuals.

KEYWORDS

autophagy stimulation, biomechanics, carbamazepine treatment, diseases and disorders of bone, micro-computed tomography, osteogenesis imperfecta, synchrotron-based Fourier-transform infrared microspectroscopy

1 | INTRODUCTION

The inherited brittle bone disease osteogenesis imperfecta (OI) is commonly caused by mutations that compromise the biosynthesis or structure of type I collagen, the predominant organic structural

component of bone. The two collagen I α -chain subunits, $\alpha 1(I)$ and $\alpha 2(I)$, which form the $[\alpha 1(I)]_2\alpha 2(I)$ collagen protein trimers are encoded by *COL1A1* and *COL1A2*. Autosomal dominant mutations in these genes cause more than 85% of OI cases^{1,2} and fall into two broad functional groups. Mutations that reduce collagen I

Natalie A. Sims and John F. Bateman joint senior authors.

This is an open access article under the terms of the [Creative Commons Attribution](https://creativecommons.org/licenses/by/4.0/) License, which permits use, distribution and reproduction in any medium, provided the original work is properly cited.

© 2022 The Authors. *Journal of Cellular and Molecular Medicine* published by Foundation for Cellular and Molecular Medicine and John Wiley & Sons Ltd.

expression, such as nonsense mutations which lead to mRNA decay, result in milder clinical phenotypes (e.g. OI type I), whereas mutations introducing missense changes causing structural disruptions in collagen pro α -chains lead to more severe OI phenotypes (e.g. OI types II, III, IV). These severe phenotypes most commonly exhibit impaired collagen I triple helix structure and stability, usually caused by glycine substitutions that interrupt the obligatory Gly-X-Y amino acid repeat sequence required for collagen helix folding. A common consequence is dysregulated collagen proteostasis, with intracellular retention and aggregation of the misfolded collagen.³ Its intracellular accumulation can induce an endoplasmic reticulum (ER) stress response which might contribute to the pathology.^{2,4}

A mouse model of OI type IV (*Col1a2*^{+/*p.G610C*}) with a Gly to Cys *Col1a2* missense mutation in the triple helix, based on an Old Order Amish OI mutation,⁵ provides us with an experimental tool for pre-clinical therapeutic testing. Previous studies on this mouse model have shown that, as expected, the glycine substitution mutation leads to intracellular mutant collagen accumulation, a poorly characterized non-canonical ER stress response and downstream impairment in osteoblast differentiation and function⁶ with clinically relevant changes to bone structure and fragility.⁷

While the molecular detail of how helix-disrupting OI mutations cause intracellular ER stress and bone pathology are not fully resolved,⁸ a promising therapeutic approach would be to reduce the load of toxic misfolded collagen and thereby reduce the OI bone pathology to a milder phenotype. There are few FDA-approved drugs that could be re-purposed to achieve this. Rapamycin, which stimulates autophagy via the mTOR pathway, showed promise on osteoblasts from the *Col1a2*^{+/*p.G610C*} mouse in vitro.⁶ However, in vivo testing in the *Col1a2*^{+/*p.G610C*} mouse demonstrated that while some OI bone trabecular properties were improved, off-target effects suppressing longitudinal and transverse bone growth in OI mice precluded rapamycin as a viable therapeutic option.⁹ Another drug stimulating mTOR-independent autophagy, carbamazepine (CBZ), has been effective in a mouse model of metaphyseal chondrodysplasia, type Schmid (MCDS), where intracellular accumulation of misfolded mutant collagen X causes ER stress and downstream pathological signalling.¹⁰ CBZ-stimulated degradation reduced the toxic mutant collagen load and ER stress, and improved the MCDS cartilage and bone pathology.^{11,12} As a result, CBZ is now in clinical trials with MCDS patients (mcds-therapy.eu). Because of the broad similarity of the molecular phenotypes in OI and MCDS (collagen misfolding and intracellular retention) and the predicted therapeutic effect of CBZ in stimulating autophagic clearance of misfolded collagen I, there is considerable interest in CBZ as a potential OI therapy.

Here, we treated 3-week-old *Col1a2*^{+/*p.G610C*} and control mice with CBZ for 3 and 6 weeks from weaning and assessed structure and strength of the long bones. While CBZ treatment for 3 weeks does not affect control bone, longer term treatment (6 weeks) during this period of active bone growth reduces bone length, width and strength. Furthermore, CBZ treatment for 3 or 6 weeks does not rescue the OI bone phenotype in *Col1a2*^{+/*p.G610C*} mice.

2 | MATERIALS AND METHODS

Heterozygous $\alpha 2(I)$ -G610C mice (*Col1a2*^{+/*p.G610C*})⁵ were obtained from Jackson Laboratory, Bar Harbour, ME, USA (B6.129[FVB]-*Col1a2*^{tm1Mcbrr/J}; stock 007248) and maintained on a C57BL/6J background to generate heterozygous *Col1a2*^{+/*p.G610C*} and control experimental mice. Mice husbandry and health monitoring are previously described.⁹ All procedures were approved by the Murdoch Children's Research Institute Animal Ethics Committee (#A798). Male control and *Col1a2*^{+/*p.G610C*} mice were treated by oral gavage with CBZ (250 mg/kg/day) from 3 to 6 weeks.^{11,12} A second cohort was additionally treated from 6 to 9 weeks by subcutaneous implantation of a slow-release pellet of carbamazepine (250 mg/kg/day) (Innovative Research of America USA C-113).¹¹ At 6 and 9 weeks, mice were euthanased and tissues harvested.

2.1 | Micro-computed tomography (μ CT)

Femora were assessed on a Skyscan 1276 micro-CT system (Bruker) at 9 micron voxel resolution as previously described,⁹ using NRecon (version 1.7.1.0), DataViewer (version 1.5.4) and CT Analyser (version 1.16.4.1). Trabecular bone structure and multi-level thresholding were carried out in the metaphysis, starting at 7.5% of bone length from the distal femoral growth plate and along 15% of total bone length. Cortical structure was assessed in the diaphysis, starting at 30% of bone length from the distal femoral growth plate and along 15% of total bone length. Medio-lateral widths and cranio-caudal widths were determined at the femoral midpoint. Single thresholds for cortical bone were 0.487 and 0.786 g/cm³ CaHA for 6- and 9-week-old mice, respectively, and for trabecular bone 0.219 and 0.435 g/cm³ CaHA for 6- and 9-week-old mice, respectively. To segregate bone into multiple density levels, nonparametric unsupervised 4 level Otsu-thresholding algorithm was used, as previously described.¹³ Each density area was normalized to total bone area, and thresholds of 0.301–0.613, 0.614–1.003 and >1.003 mg/cm² CaHA were used for low-, mid- and high-density bone areas, respectively; the background level (0–0.3 mg.cm² CaHA) was discarded.

2.2 | Three point bending strength tests

After μ CT, femora were stored in 70% ethanol. Three point bending was performed with a Bose Biodynamic 5500 Test instrument (Bose, DE, USA) and WinTest 7 software. Femora were centred onto supporting pins with a span width of 6 mm and loaded with 0.5 mm/s. As described previously,¹⁴ the load/deformation data were collected over 5 s with a sampling rate of 250 Hz. For material properties, the data were normalized to medio-lateral and cranio-caudal widths and average cortical thickness of the diaphysis of each bone.

2.3 | Synchrotron-based Fourier-transform infrared microspectroscopy (sFTIRM)

sFTIRM was conducted on a Bruker Hyperion 2000 IR microscope coupled to a V80v FTIR spectrometer at the Australian Synchrotron IR Microspectroscopy beamline, as previously described.¹⁵ Briefly, 2 μm undecalcified methyl methacrylate (MMA) embedded tibial sections¹⁶ were placed on 0.5 mm barium fluoride windows (Crystan Limited), and 16 \times 16 μm regions of interest were measured with 10 μm spacing from the periosteal edge at 1.5 mm proximal to the growth plate in the medial cortex. Spectra were collected using a wideband detector with 256 co-added scans per pixel spectral resolution in transmission mode. For each sample, background spectra were collected through both clear barium fluoride and MMA. Data acquisition and analysis were performed with Bruker OPUS version 8.0. To analyse the raw spectra, each spectrum was corrected for water vapour, baseline corrected at 1800, 1200 and 800 cm^{-1} and absorbed MMA was subtracted. Bone composition was determined by integrating areas as follows: mineral: matrix ratio using amide I (1180–916:1712–1588 cm^{-1}) or amide II (1180–916:1600–1500 cm^{-1}), carbonate substitution (890–852:1180–916 cm^{-1}) and collagen compaction (1712–1588:1600–1500 cm^{-1}) and crystallinity from 1030 to 1020 cm^{-1} , all as previously described.^{15,17}

2.4 | Statistical analysis

All graphs show mean \pm SEM. Sample number (n) is indicated in figure legends. Statistical significance was calculated with GraphPad Prism 9 (version 9.1.2.) by two-way ANOVA and Tukey's multiple comparison test for all comparisons except for the regional analysis for sFTIRM and Otsu thresholding where two-stage linear step-up procedure of Benjamini, Krieger and Yekutieli was used.

3 | RESULTS

3.1 | Six-week-old *Col1a2*^{+p.G610C} mice have defective bone structure that is not modified by CBZ treatment from 3 weeks of age

Previous studies have shown that from 8 weeks of age (but not at 10 days of age), *Col1a2*^{+p.G610C} mice have less cortical and trabecular bone and lower bone strength than controls.^{5,7,9,18} We showed that the phenotype can also be detected at 6 weeks of age. Femora from 6-week-old vehicle-treated *Col1a2*^{+p.G610C} mice were narrower with significantly lower cortical area, periosteal and endocortical perimeters compared to controls (Figure 1A–D). In addition, the marrow area, mean polar moment of inertia and medio-lateral and cranio-caudal widths were significantly lower than controls (Table S1). *Col1a2*^{+p.G610C} femora from 6-week-old mice also had significantly lower trabecular bone volume, number, separation and shorter femora than controls (Figure 1E–I). Treatment with 250 mg/kg/day CBZ

for 3 weeks, a dose equivalent to that used in treating epilepsy in human subjects taking into account species differences¹⁹ and to correct cartilage defects in the MCDS mouse,^{11,12} did not significantly modify cortical or trabecular bone mass in either control or *Col1a2*^{+p.G610C} femora (Figure 1A–I; Table S1).

3.2 | CBZ from 3 to 9 weeks of age had no effect in *Col1a2*^{+p.G610C} mice but impaired bone growth in control mice

The lower trabecular bone mass, and smaller femoral length and width of 6-week-old vehicle-treated *Col1a2*^{+p.G610C} mice compared to controls were also detected at 9 weeks of age (Figure 2; Table S2). The extended period of CBZ treatment (from 3 to 9 weeks of age) had no significant effect on trabecular or cortical structure in *Col1a2*^{+p.G610C} femora (Figure 2; Table S2). Although short-term CBZ treatment in control mice for 3 weeks had no effect on bone structure (Figure 1; Table S1), a longer duration of CBZ treatment for 6 weeks led to significantly lower cortical area, cortical thickness, periosteal and endocortical perimeters (Figure 2A–D), marrow area, mean polar moment of inertia, medio-lateral and cranio-caudal widths (Table S2), indicating suppressed transverse bone growth. Six weeks of CBZ treatment in control mice lowered trabecular bone volume, thickness and number (Figure 2E, F, H). In these 9-week-old mice, trabecular thickness and number were lower than in the younger vehicle-treated control mice (Figure 1E, F, H), suggesting loss of trabecular bone mass, rather than impaired trabecular bone accrual. In addition, while femoral length was greater at 9 weeks than 6 weeks in vehicle-treated control mice, CBZ-treated control mice had shorter femora than vehicle-treated controls (Figures 1I and 2I), indicating that a longer duration of CBZ treatment suppressed both transverse and longitudinal bone growth.

3.3 | *Col1a2*^{+p.G610C} mice have disrupted cortical bone consolidation, but this is modified by CBZ only in control mice

Cortical bone consolidates by changing from a material with a high proportion of low-density bone to a material with mainly high-density bone.¹⁶ This transition can be measured along the length of the growing bone from the growth plate (more low-density bone) to the diaphysis (more high-density bone). Since cortical diaphyseal bone of *Col1a2*^{+p.G610C} mice has greater average tissue mineral density,¹⁸ we used multi-level thresholding to assess whether high-density material accrued more rapidly in less mature regions of the femoral metaphysis of *Col1a2*^{+p.G610C} mice.

When total proportions of low-, mid- and high-density bone were assessed in vehicle-treated animals, *Col1a2*^{+p.G610C} femora had a higher proportion of mid-density bone material than controls, with no significant difference in proportions of low- or high-density bone (Figure 3). This was not modified by CBZ treatment (Figure 3).

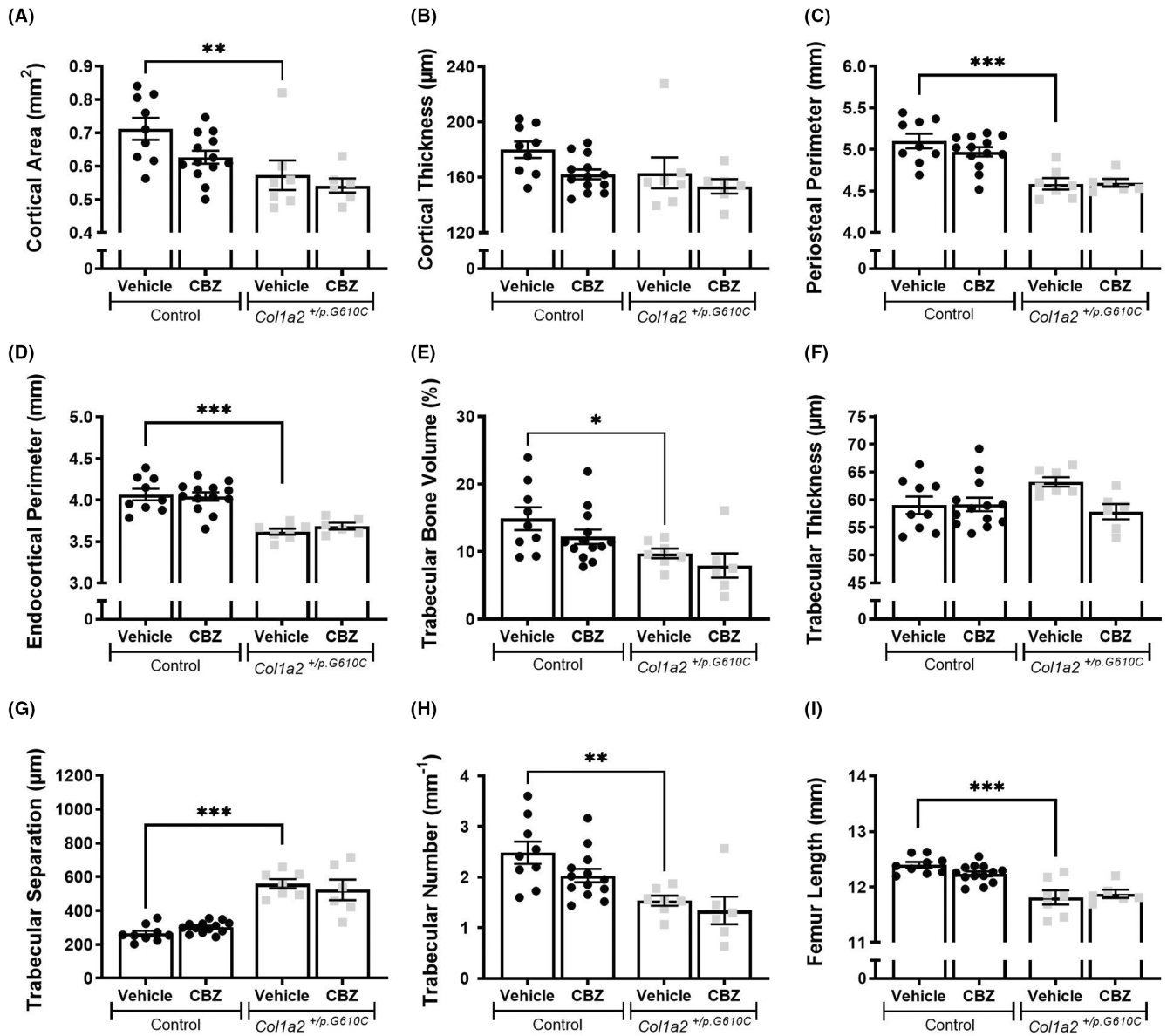


FIGURE 1 Femoral bone structure of 6-week-old male control and *Col1a2*^{+/p.G610C} mice treated with vehicle or carbamazepine (CBZ) for 3 weeks assessed by micro-computed tomography (μ CT). Shown are (A) cortical area, (B) cortical thickness, (C) periosteal perimeter and (D) endocortical perimeter, (E) trabecular bone volume, (F) trabecular thickness, (G) trabecular separation, (H) trabecular number and (I) femur length from male control and *Col1a2*^{+/p.G610C} mice. Data shown are mean \pm SEM, $n = 6$ –13 mice/group. * $p < 0.05$, ** $p < 0.01$, *** $p < 0.001$ vs. treatment-matched controls

When assessed along the length of the bone, vehicle-treated control and *Col1a2*^{+/p.G610C} bones both showed the expected reduction in low-density and increase in high-density bone with increasing distance from the growth plate (Figure S1A). However, *Col1a2*^{+/p.G610C} bones had less high-density bone in the least mature region (close to the growth plate), more low-density bone in the most mature region (near the diaphysis) and a higher proportion of mid-density bone along the full length of the metaphysis, indicating region-specific differences in cortical bone maturation in this model of OI.

CBZ treatment from 3 to 9 weeks of age increased the proportion of high-density bone and reduced the proportion of low-density bone in control mice (Figure 3). This was significant along the full extent of

the metaphysis, indicating that it existed at all stages of cortical bone consolidation and that CBZ could change the type of bone deposited (Figure S1B). CBZ treatment did not affect these parameters in *Col1a2*^{+/p.G610C} femora at any point along the metaphysis (Figure S1C).

3.4 | sFTIRM shows mineral: matrix content of *Col1a2*^{+/p.G610C} bone progressively increases in deeper sub-periosteal bone

Eight-week-old, but not 10 day old, male *Col1a2*^{+/p.G610C} mice exhibit high mineral: matrix ratio,⁷ consistent with an imbalance between

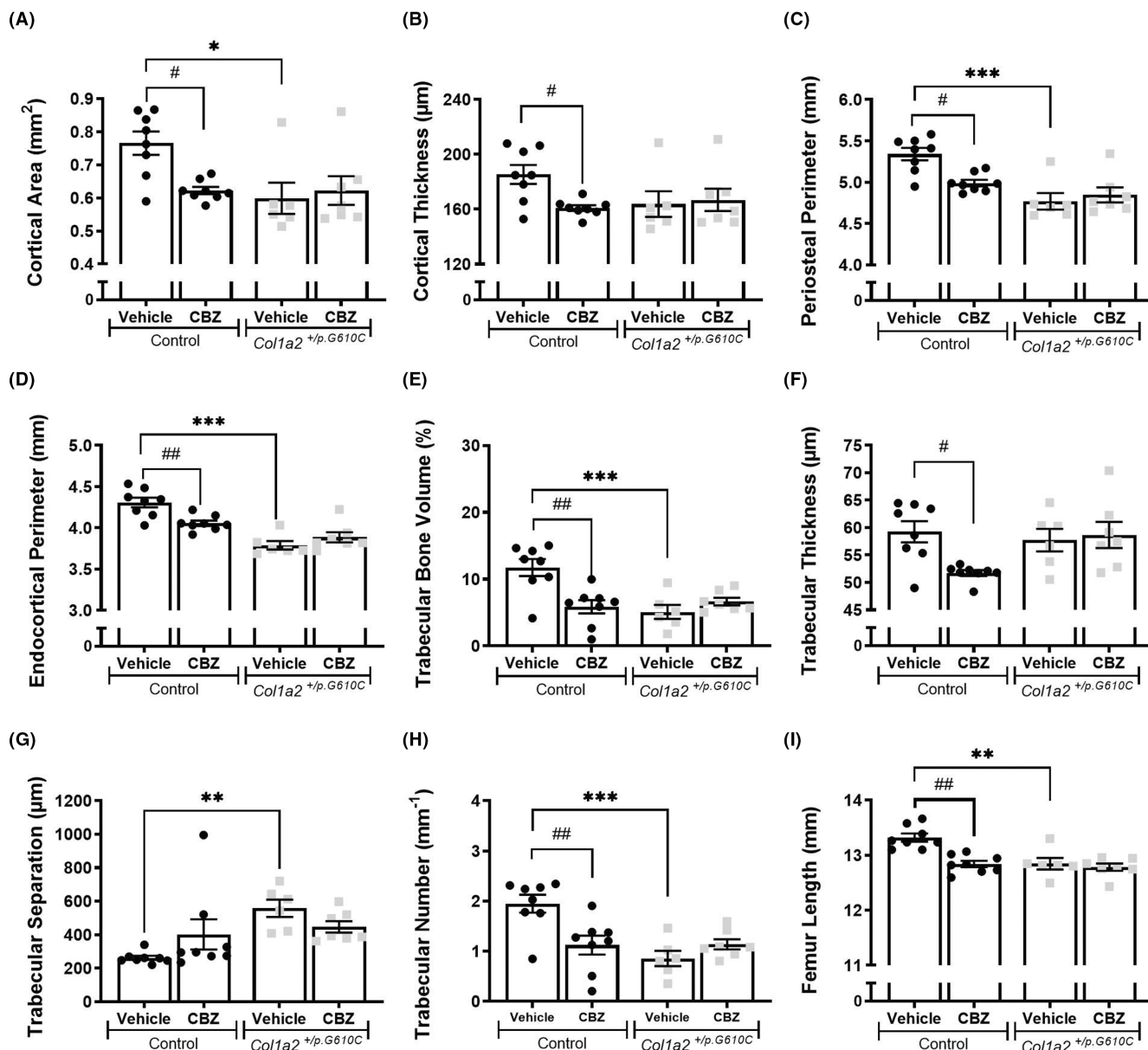


FIGURE 2 Femoral bone structure of 9-week-old male control and *Col1a2*^{+/p.G610C} mice treated with vehicle or carbamazepine (CBZ) for 6 weeks assessed by micro-computed tomography (μ CT). Shown are (A) cortical area, (B) cortical thickness, (C) periosteal perimeter and (D) endocortical perimeter, (E) trabecular bone volume, (F) trabecular thickness, (G) trabecular separation, (H) trabecular number and (I) femur length from male control and *Col1a2*^{+/p.G610C} mice. Data shown are mean \pm SEM, $n = 6-8$ mice/group. * $p < 0.05$, ** $p < 0.01$, *** $p < 0.001$ vs. treatment-matched controls. # $p < 0.5$, ## $p < 0.01$ vs. genotype-matched controls

collagen production and mineral accrual.²⁰ Since 12-week-old tibial cortex exhibits a gradient of matrix maturation from the periosteal edge moving inwards, including mineral accrual, collagen compaction and carbonate substitution,^{15,17} we assessed whether the OI phenotype or CBZ treatment modified bone matrix composition and maturation.

Both 6- and 9-week-old vehicle-treated *Col1a2*^{+/p.G610C} tibial cortex had greater mineral: matrix ratio (higher phosphate: amide I ratio) than controls (Figure 4A,C), indicating that this matrix defect is already significant at 6 weeks of age. In vehicle-treated animals, the mineral: matrix ratio increased in both control and *Col1a2*^{+/p.G610C} bone at 10 μ m and 20 μ m inwards from

the periosteal edge compared to the periosteum, at both 6 and 9 weeks of age; the slope of this increase was notably greater in the more mature 9-week-old bone (Figure 4B,D). Additionally, 6-week-old *Col1a2*^{+/p.G610C} bones had a higher mineral: matrix ratio at 10 μ m and, in 9-week-old mice, at both 10 μ m and 20 μ m from the periosteum compared to the same regions in control bones (Figure 4B,D). The mineral: matrix ratio using the amide II reference showed a similar response (Table 1; Figure S2A,E). This indicates that although mineral is initially deposited at normal levels on the growing periosteum of *Col1a2*^{+/p.G610C} bones, it accrues mineral more rapidly in *Col1a2*^{+/p.G610C} mice than in controls.

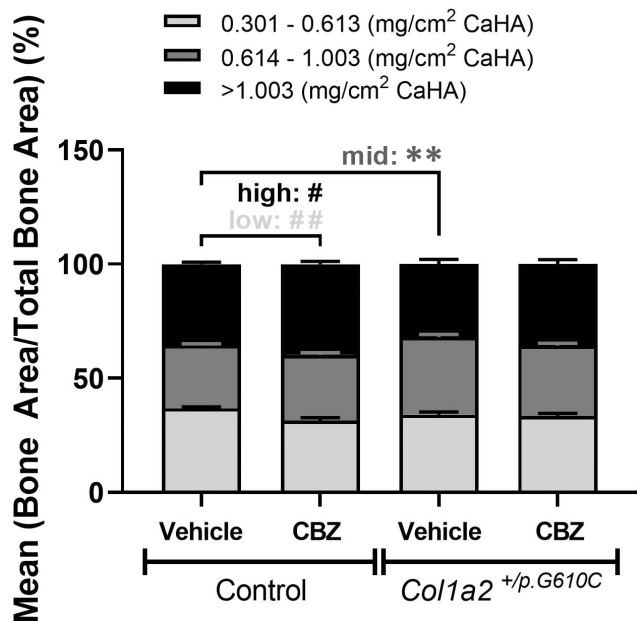


FIGURE 3 Multi-level-thresholding analysis of the average femoral metaphysis segregated by low- (light-grey), mid- (dark-grey) and high-density (black) levels of the femoral cortex from 9-week-old male control and *Col1a2*^{+/p.G610C} mice treated with vehicle or carbamazepine (CBZ) for 6 weeks by micro-computed tomography (μ CT). Data are mean \pm SEM; $n = 5-8$ mice/group. $**p < 0.01$ vs. treatment-matched controls. $\#q < 0.05$, $\#\#q < 0.01$ vs. treatment- and region-matched controls

Average crystallinity and amide I:II ratio (collagen compaction) were not significantly different between vehicle-treated control and *Col1a2*^{+/p.G610C} bone at 6 or 9 weeks of age (Table 1). Although carbonate:phosphate ratio was lower in vehicle-treated *Col1a2*^{+/p.G610C} bones than control at 6 weeks of age (Table 1), this genotype-dependent effect was not observed at 9 weeks of age. While average carbonate:phosphate ratio was lower in vehicle-treated *Col1a2*^{+/p.G610C} than controls at 6 weeks of age, region-specific analysis showed no change in carbonate:phosphate ratios with matrix maturation in either controls or *Col1a2*^{+/p.G610C} bones at any age (Figure S2B,F). However, average crystallinity increased and amide I:II ratio decreased with increasing distance from the periosteum in both genotypes at 9 weeks of age (Figure S2G,H), suggesting that *Col1a2*^{+/p.G610C} bone undergoes normal mineral maturation at 9 weeks of age, apart from the abnormal increase in mineral relative to collagen. No significant effects of CBZ were detected by sFTIRM in either control or *Col1a2*^{+/p.G610C} mice (Figure 4; Figure S2A-H; Table 1).

3.5 | CBZ does not improve the *Col1a2*^{+/p.G610C} bone strength defect but reduces bone strength in control mice

Three point bending tests in vehicle-treated mice showed that femora from 6- and 9-week-old *Col1a2*^{+/p.G610C} mice were weaker than control femora (Figure 5). This difference was greater in

9-week-old mice, which showed a ~60% lower maximum load than controls (Figure 5E) while 6-week-old *Col1a2*^{+/p.G610C} femora were only ~30% weaker than their age-matched controls (Figure 5A). *Col1a2*^{+/p.G610C} femora were also more brittle compared to control femora, and again, this was more pronounced in 9-week-old mice, shown by a ~90% lower post yield displacement (Figure 5F). There were also greater differences between the genotypes in yield load (Tables S1 and S2) in 9-week-old than 6-week-old mice.

Since *Col1a2*^{+/p.G610C} femurs were narrower than controls, strength testing data were corrected for bone widths and cortical thickness. When corrected for bone size, vehicle-treated *Col1a2*^{+/p.G610C} femora were still more brittle than controls at both ages, shown by a lower post yield strain (Figure 5D,H), and lower elastic deformation, shown by a lower yield strain (Tables S1 and S2). The stiffness of *Col1a2*^{+/p.G610C} femora was double that of controls, shown by a higher elastic modulus (Table S2). There was no difference in maximum stress in *Col1a2*^{+/p.G610C} femora compared to control femora (Figure 5C) at 6 weeks of age but a significant reduction at 9 weeks (Figure 5G). This suggests that the genotype-dependent reduction in bone strength at 6 weeks can be explained by the smaller size but the bone strength defect persists in 9-week-old mice due to the progressing material defect. This indicates that the OI phenotype progressively worsens between 6 and 9 weeks of age.

CBZ had no significant effect on any parameter measured by three point bending tests in *Col1a2*^{+/p.G610C} mice at 6 or 9 weeks of age (Figure 5; Table S1 and S2). However, in control mice, although 3 weeks of CBZ treatment did not modify bone strength, after 6 weeks of treatment maximum load, yield load and displacement were significantly lower than in vehicle-treated controls (Figure 5A,E; Tables S1 and S2). When corrected for bone width, no strength parameters were significantly altered by either 3 or 6 weeks of CBZ treatment (Figure 5C,D,G,H; Tables S1 and S2). This indicates that CBZ treatment of 3-week-old control mice for 6 weeks suppresses bone growth sufficiently to reduce functional strength.

4 | DISCUSSION

This study was based on the premise that stimulation of autophagic mutant collagen I degradation by carbamazepine (CBZ) treatment might provide therapeutic benefit in OI. In collagen misfolding disorders, the best evidence for this approach comes from a mouse model of Metaphyseal Chondrodysplasia, Type Schmid (MCDS), where CBZ treatment stimulated autophagic degradation of the mutant misfolded collagen X, reducing ER stress and improving the cartilage and bone disease severity.^{11,12} This provided a strong rationale for testing the possible therapeutic effect of carbamazepine in the *Col1a2*^{+/p.G610C} mouse model of OI. However, we found that treatment of 3-week-old *Col1a2*^{+/p.G610C} mice for either 3 or 6 weeks with CBZ, at the dose effective in the MCDS model, had no therapeutic benefit for the deficiencies in

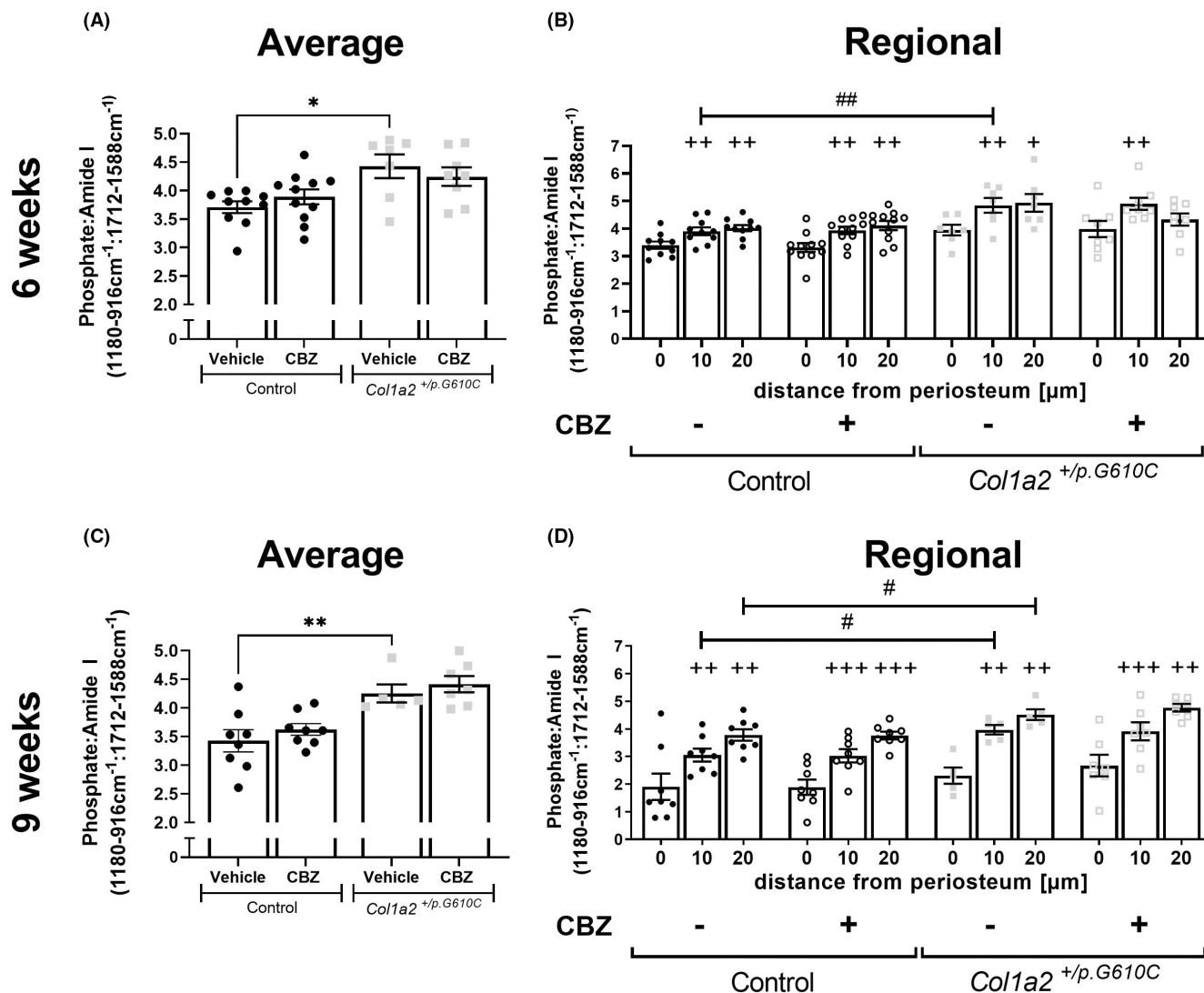


FIGURE 4 Analysis of average (A,C) and regional (B,D) mineral: matrix ratios of tibial cortex from 6-week-old (A,B) and 9-week-old (C,D) male control and *Col1a2*^{+p.G610C} mice treated with vehicle or carbamazepine (CBZ) for 3 or 6 weeks, respectively, by synchrotron Fourier-transform infrared microspectroscopy (sFTIRM). Data are shown as the average phosphate: amide I ratio and regional measurements, which show data at 10 micron intervals with increasing distance from the periosteum. Ratios were calculated from integrated areas of phosphate (1180–916 cm^{-1}) and amide I (1712–1588 cm^{-1}) curves. Data are mean \pm SEM; $n = 7$ –11 mice/group for 6-week-old mice and $n = 5$ –8 mice/group for 9-week-old mice. * $p < 0.05$, ** $p < 0.01$ vs. treatment-matched controls. + $q < 0.05$, ++ $q < 0.01$, +++ $q < 0.001$ vs. genotype- and treatment-matched region 0 μm . # $q < 0.05$, ## $q < 0.01$ vs. treatment- and region-matched controls

bone structure, strength or composition in *Col1a2*^{+p.G610C} mice. The study also provides new information about the *Col1a2*^{+p.G610C} mouse bone phenotype and reveals that CBZ treatment in mice with healthy skeletons can be detrimental.

The lack of beneficial effect of CBZ on *Col1a2*^{+p.G610C} bone is not due to unavailability of CBZ in the OI bone with this treatment regime, since the impact of CBZ on the control bone (discussed below) clearly indicates that the CBZ was bio-available in these growing bones. Furthermore, this dose of CBZ was effective in modifying the ER stress response of the MCDS mouse growth plate cartilage.^{11,12} This suggests that CBZ does not stimulate sufficient intracellular clearance of mutant misfolded/aggregated collagen I in vivo to have a positive clinical effect on downstream pathological signalling in

the *Col1a2*^{+p.G610C} bone. Furthermore, while both MCDS and OI (*Col1a2*^{+p.G610C}) are caused by mutant collagen misfolding and intracellular retention, the collagen types (collagen X and collagen I, respectively), the nature and context of the mutations are different,^{6,10} perhaps requiring different strategies to remove accumulated protein from the affected cells.

This is the second study showing that autophagy-stimulating drugs do not improve bone structure or strength in the *Col1a2*^{+p.G610C} mouse. Other approaches based on clearing mutant collagen may still be effective, since rapamycin⁹ and CBZ have known 'off-target' effects. An alternative approach that has gained traction in several diseases is to reduce the mutant misfolded protein load, not by degradation, but by chemical chaperones such as 4-phenylbutyric acid (4-PBA) to assist

TABLE 1 Additional bone composition parameters of tibial cortex from 6-week and 9-week-old male control and *Col1a2*^{+p.G610C} mice treated with vehicle or carbamazepine (CBZ) for three and 6 weeks, respectively, by synchrotron Fourier-transform infrared microspectroscopy (sFTIRM). Ratios were calculated from integrated areas of phosphate (1180–916 cm⁻¹), carbonate (890–852 cm⁻¹), amide I (1712–1588 cm⁻¹) and amide II (1600–1500 cm⁻¹) curves. Crystallinity sub-peak was calculated by the integrated area from 1030–1020 cm⁻¹. Data shown are mean ± SEM; n = 7–11 mice/group for 6-week-old mice and n = 5–8 mice/group for 9-week-old mice. *p < 0.05, **p < 0.01, ***p < 0.01 vs. controls

	Control		<i>Col1a2</i> ^{+p.G610C}	
	Vehicle (n = 10)	CBZ (n = 11)	Vehicle (n = 7)	CBZ (n = 8)
6 weeks				
Phosphate:Amide II	6.49 ± 0.13	6.49 ± 0.08	7.52 ± 0.39**	7.22 ± 0.20
Carbonate:Phosphate	0.009 ± 0.0003	0.008 ± 0.0002	0.007 ± 0.0004*	0.008 ± 0.0002
Crystallinity	0.72 ± 0.03	0.72 ± 0.04	0.86 ± 0.06	0.76 ± 0.05
Amide I:II	1.78 ± 0.02	1.72 ± 0.04	1.72 ± 0.04	1.74 ± 0.03
	Control		<i>Col1a2</i> ^{+p.G610C}	
	Vehicle (n = 8)	CBZ (n = 8)	Vehicle (n = 5)	CBZ (n = 7)
9 weeks				
Phosphate:Amide II	5.61 ± 0.21	6.12 ± 0.17	7.14 ± 0.30***	7.01 ± 0.16
Carbonate:Phosphate	0.009 ± 0.0005	0.009 ± 0.0001	0.009 ± 0.0002	0.009 ± 0.0004
Crystallinity	0.17 ± 0.03	0.14 ± 0.03	0.13 ± 0.03	0.12 ± 0.02
Amide I:II	1.72 ± 0.04	1.76 ± 0.02	1.73 ± 0.03	1.65 ± 0.03

in refolding the mutant proteins.²¹ 4-PBA reduces ER stress *in vitro* in fibroblasts with a range of mutations, including COL1A1 and COL1A2 misfolding mutations.^{22,23} *In vivo*, 4-PBA treatment improved bone abnormalities in a zebrafish collagen helix misfolding mutation (*Col1a1a* p.G736D) OI model,²⁴ and in the *Aga2*^{+/-} mouse model, where a *Col1a1* frameshift mutation in the C-propeptide results in failed procollagen I assembly.²⁵ In contrast, in the *Col1a2*^{+p.G610C} mouse 4-PBA reduced the OI bone growth deficiency by enhancing the transition of the OI hypertrophic chondrocytes to osteoblasts, a process suppressed with this OI mutation.²⁶ 4-PBA had little, or no, impact on the OI osteoblasts and did not rescue the bone fragility phenotype.²⁷ Thus, 4-PBA may be effective for some OI mutations, less so for others, most likely due to the nature of the collagen folding defects caused by different mutations and the resulting cellular response to the misfolded collagen. The cellular response to the disturbed proteostasis resulting from collagen I misfolding, and whether a canonical or 'non-canonical' UPR results remains unclear with many mutations, especially those disturbing the triple helix.⁸ Those impacting the C-propeptide may be more likely to elicit a canonical UPR⁸ and it is tempting to speculate that CBZ may be more effective with these given their similarity to the CBZ-responsive collagen X mutations,¹¹ and the positive effect of 4-PBA on the *Aga2*^{+/-} mice.²⁵

While CBZ treatment could show mutation specificity in its effect, the use of CBZ as a OI therapeutic is, however, moot since we found that the 6-week CBZ treatment of 3-week-old growing bone in control mice was deleterious. CBZ impaired bone growth, in both longitudinal and transverse directions, and reduced the cortical and trabecular bone mass of healthy mice leading to a significant reduction in functional bone strength. Although CBZ treatment changed the morphology of the control bone to reach similar proportions to

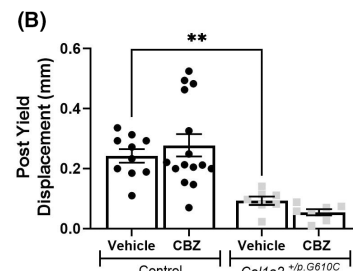
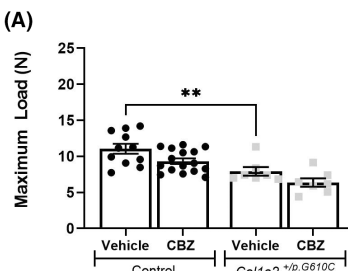
the OI bone, the strength defect caused by CBZ was less severe than the OI phenotype. This was because CBZ changed bone morphology without accompanying changes in bone composition, measured by sFTIRM. The reason why CBZ has a negative impact on control bone growth, but not the mouse OI bone, is not known. CBZ has been shown *in vitro* to inhibit both osteoclastogenesis in human peripheral blood mononuclear cell-derived osteoclast precursors and osteoblastogenesis in human mesenchymal stem cell osteoblast precursors.²⁸ Disturbance to the delicate balance of these processes during bone growth could explain the CBZ effect on control bones. In the *Col1a2*^{+p.G610C} OI mouse model, bone marrow stromal cells had a much-reduced ability to form mature osteoblasts compared to controls⁶ and *in vivo*, recent studies have shown the maturation and trans-differentiation of hypertrophic chondrocytes to osteoblasts is significantly reduced, resulting in the reduced growth of the OI bones.^{26,27} Given the already severely deficient osteoblast differentiation and reduced bone growth in the OI mouse, it seems likely that the OI bones could be less sensitive to any additional impact on osteoblast differentiation and bone growth resulting from CBZ treatment.

CBZ is a widely used anti-epileptic drug (AED), and there have been multiple reports that short- and long-term CBZ treatment in children and adults with epilepsy leads to low serum 25-hydroxyvitamin D, and high serum parathyroid hormone and alkaline phosphatase.^{29–31} This suggests CBZ, like other anti-convulsant therapies, causes osteomalacia and secondary hyperparathyroidism and may increase fracture risk.³² However, analyses of the effect of CBZ on bone structure in children with epilepsy have been limited to small observational studies, with some reporting reduced areal bone mineral density (BMD)^{30,33} but others indicating no significant effect.^{34–37} No studies have reported

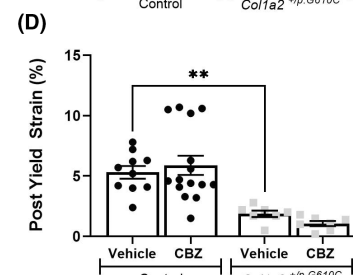
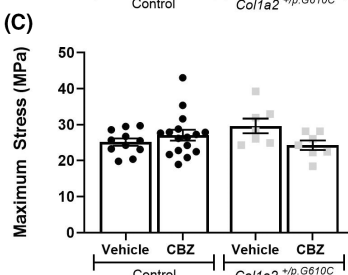
FIGURE 5 Results of three point bending tests, including raw data (structural properties) and those corrected for bone size (material properties) of femora from 6-week and 9-week-old male control and *Col1a2*^{+p.G610C} mice treated with vehicle or carbamazepine (CBZ) for three and six weeks, respectively. Shown are (A) maximum load, (B) post-yield displacement, (C) maximum stress and (D) post-yield strain of femora from 6-week-old control and *Col1a2*^{+p.G610C} mice and (E) maximum load, (F) post-yield displacement, (G) maximum stress and (H) post-yield strain of femora from 9-week-old control and *Col1a2*^{+p.G610C} mice. Data shown are mean \pm SEM, $n = 7$ –16 mice/group for 6-week-old mice and $n = 6$ –8 mice/group for 9-week-old mice. * $p < 0.05$, ** $p < 0.01$, *** $p < 0.001$ vs. treatment-matched controls. # $p < 0.05$ vs. genotype-matched controls

6 weeks

Structural properties

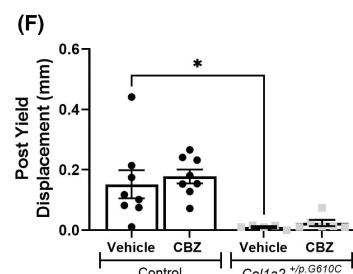
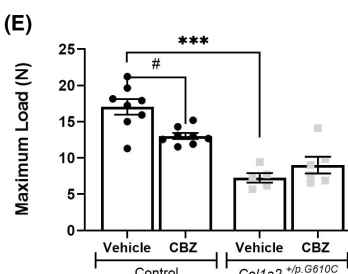


Material properties

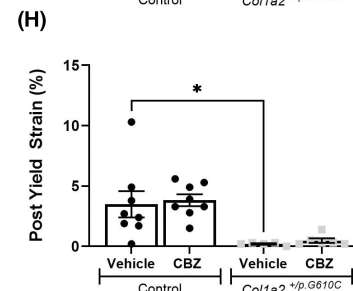
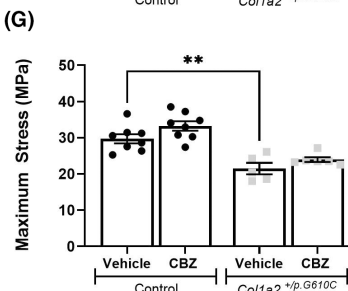


9 weeks

Structural properties



Material properties



how CBZ in children influences bone growth. Pre-clinical studies have been limited to adult rats, and these too have conflicting results, with one study reporting no change in cortical or trabecular structure by micro-CT, nor any change in bone strength,³⁸ but another reporting a significant decline in both trabecular bone mass and BMD at multiple sites.³⁹ It will be important to systematically evaluate any effects of CBZ on normal bone structure and biomechanics to resolve the conflicting data and inform on the importance of further studies on CBZ as a potential OI therapy.

A limitation of our study was that it was conducted only on male mice. A recent detailed study of the morphological and mechanical phenotypes of the bone in *Col1a2*^{+p.G610C} mice showed that the OI defects were similar in mice of both sexes.¹⁸ It is a reasonable expectation that a therapeutic targeting a fundamental process, such as CBZ-induction of autophagy, would work in both male and female mice, albeit possibly to different extents because of sex-dependent skeletal variation. If we had found a therapeutic benefit from CBZ in

this study, it would be important to repeat these studies on female mice to look further at the sex dependence of drug dosage and therapeutic regime.

This study also provides new information about the OI phenotype. Firstly, it shows that this phenotype can be detected as early as 6 weeks of age, a time point not previously studied, and that the defect in bone strength becomes more severe by 9 weeks of age. Our data suggest that the phenotype progression between 6 and 9 weeks of age is largely due to a worsening material defect. There are three pieces of evidence for this: (1) the difference in cortical bone size and shape between control and *Col1a2*^{+p.G610C} bones did not worsen with age, (2) the defective mineral: matrix ratio did become more severe with age, and (3) the worsening difference in bone strength persists after correcting for bone size

Our work also provides new information about defects in skeletal maturation in the *Col1a2*^{+p.G610C} mouse. Bone undergoes multiple changes in post-embryonic growth. Not only do the bones

lengthen, but cortical bone thickens, and the material changes from woven bone to an increasingly dense lamellar structure^{40,41}; this is reflected in the micro-CT scans showing a transition with increasing distance from the growth plate from a high proportion of low-density bone to a material containing more high-density bone.^{13,16} *Col1a2*^{+p.G610C} femora did exhibit cortical bone maturation, but the presence of less high-density bone in the least mature region (close to the growth plate), and more low-density bone in the most mature region (near the diaphysis), could indicate an initial more rapid process of cortical maturation and an early plateau, such that there is a higher proportion of mid-density bone along the full metaphyseal length. Our sFTIRM analysis also indicates that the greater proportion of mineral relative to collagen in *Col1a2*^{+p.G610C} bone is already significant at 6 weeks of age and is only detected in more mature regions of bone. This indicates that although mineral is initially deposited at normal levels on the periosteum of *Col1a2*^{+p.G610C} bone matrix, it accrues more rapidly in these mice than controls, probably driven by the defective collagen structure.

Our data raise two important considerations for any future applications of CBZ in genetic skeletal disease therapy. Firstly, given the lack of effect with this *Col1a2*^{+p.G610C} mutant, it seems unlikely that CBZ will be useful for broad-based OI therapy. It remains possible that a beneficial CBZ effect could be OI mutant-specific, but this would require extensive mutation-specific testing in patients. Secondly, and more importantly, the negative impact of CBZ on normal bone growth and structure is worrying in terms of any proposed therapies. If experimental evidence emerges that CBZ is beneficial with specific protein misfolding mutations, it will be critically important to closely monitor bone growth in clinical trials to ensure that any potential benefits outweigh the possible side effects. This may be particularly important when treatment coincides with bone growth.

AUTHOR CONTRIBUTIONS

Martha Blank: Data curation (equal); formal analysis (equal); investigation (equal); writing – original draft (equal); writing – review and editing (equal). **Narelle McGregor:** Investigation (equal); writing – review and editing (equal). **Lynn Rowley:** Investigation (equal); writing – review and editing (equal). **Louise Kung:** Investigation (equal); writing – review and editing (equal). **Blessing Crimeen-Irwin:** Investigation (equal); writing – review and editing (equal). **Ingrid Poulton:** Investigation (equal); writing – review and editing (equal). **Emma McGowan:** Investigation (equal); writing – review and editing (equal). **Jonathan Gooi:** Investigation (equal); writing – review and editing (equal). **Shireen Lamandé:** Conceptualization (equal); funding acquisition (equal); project administration (equal); writing – review and editing (equal). **Natalie A Sims:** Conceptualization (equal); formal analysis (equal); funding acquisition (equal); project administration (equal); resources (equal); supervision (equal); writing – original draft (equal); writing – review and editing (equal). **John Bateman:** Conceptualization (equal); formal analysis (equal); funding acquisition (equal); project administration (equal); resources (equal); supervision (equal); writing – original draft (equal); writing – review and editing (equal).

ACKNOWLEDGEMENTS

This study was funded by an Australian National Health & Medical Research Council project grant (GNT 1049863) and Senior Research Fellowship (GNT 1154819) (to N.A.S.), philanthropic support to St. Vincent's Institute, and the Victorian Government's Operational Infrastructure Support Program. The FTIRM data were generated on the IRM beamline at the Australian Synchrotron, part of ANSTO, and we thank Pimm Vongsvivut and Mark Tobin for their assistance there; we also thank Mark Forwood, Griffith University, for consulting on the mechanical testing method.

CONFLICT OF INTEREST

The authors declare no conflicts of interest.

DATA AVAILABILITY STATEMENT

Data available on request from the authors

ORCID

John F. Bateman  <https://orcid.org/0000-0001-8542-0730>

REFERENCES

- Forlino A, Marini JC. Osteogenesis imperfecta. *Lancet*. 2016;387(10028):1657-1671.
- Bateman JF, Boot-Handford RP, Lamandé SR. Genetic diseases of connective tissues: cellular and extracellular effects of ECM mutations. *Nat Rev Genet*. 2009;10(3):173-183.
- Ishida Y, Yamamoto A, Kitamura A, et al. Autophagic elimination of misfolded procollagen aggregates in the endoplasmic reticulum as a means of cell protection. *Mol Biol Cell*. 2009;20(11):2744-2754.
- Boot-Handford RP, Briggs MD. The unfolded protein response and its relevance to connective tissue diseases. *Cell Tissue Res*. 2010;339(1):197-211.
- Daley E, Streeten EA, Sorkin JD, et al. Variable bone fragility associated with an Amish COL1A2 Variant and a Knock-in Mouse model. *J Bone Min Res*. 2010;25(2):247-261.
- Mirigian LS, Makareeva E, Mertz EL, et al. Osteoblast malfunction caused by cell stress response to procollagen misfolding in $\alpha 2(I)$ -G610C mouse model of osteogenesis imperfecta. *J Bone Miner Res*. 2016;31(8):1608-1616.
- Masci M, Wang M, Imbert L, et al. Bone mineral properties in growing *Col1a2*^{+p.G610C} mice, an animal model of osteogenesis imperfecta. *Bone*. 2016;87:120-129.
- Bateman JF, Shoulders MD, Lamandé SR. Collagen misfolding mutations: the contribution of the unfolded protein response to the molecular pathology. *Connect Tissue Res*. 2022;63(3):210-227.
- Bateman JF, Sampurno L, Maurizi A, et al. Effect of rapamycin on bone mass and strength in the $\alpha 2(I)$ -G610C mouse model of osteogenesis imperfecta. *J Cell Mol Med*. 2019;23(3):1735-1745.
- Rajpar MH, McDermott B, Kung L, et al. Targeted induction of endoplasmic reticulum stress induces cartilage pathology. *PLoS Genet*. 2009;5(10):e1000691.
- Mullan LA, Mularczyk EJ, Kung LH, et al. Increased intracellular proteolysis reduces disease severity in an ER stress-associated dwarfism. *J Clin Invest*. 2017;127(10):3861-3865.
- Forouhan M, Sonntag S, Boot-Handford RP. Carbamazepine reduces disease severity in a mouse model of metaphyseal chondrodysplasia type Schmid caused by a premature stop codon (Y632X) in the *Col10a1* gene. *Hum Mol Genet*. 2018;27(22):3840-3853.

13. Walker EC, McGregor NE, Chan ASM, Sims NA. Measuring bone volume at multiple densities by micro-computed tomography. *Bio Protoc.* 2021;11(1):e3873.
14. Williamson L, Hayes A, Hanson ED, Pivonka P, Sims NA, Gooi JH. High dose dietary vitamin D3 increases bone mass and strength in mice. *Bone Rep.* 2017;6:44-50.
15. Vrahnas C, Pearson TA, Brunt AR, et al. Anabolic action of parathyroid hormone (PTH) does not compromise bone matrix mineral composition or maturation. *Bone.* 2016;93:146-154. doi:10.1016/j.bone.2016.09.022
16. McGregor NE, Poulton IJ, Walker EC, Sims NA. Testing Bone Formation Induction by Calvarial Injection Assay in vivo. *Bio Protoc.* 2020;10(6):e3560.
17. Vrahnas C, Blank M, Dite TA, et al. Increased autophagy in EphrinB2-deficient osteocytes is associated with elevated secondary mineralization and brittle bone. *Nat Commun.* 2019;10(1):3436.
18. Kohler R, Tastad CA, Creecy A, Wallace JM. Morphological and mechanical characterization of bone phenotypes in the Amish G610C murine model of osteogenesis imperfecta. *PLoS One.* 2021;16(8):e0255315.
19. Nair AB, Jacob S. A simple practice guide for dose conversion between animals and human. *J Basic Clin Pharm.* 2016;7(2):27-31.
20. Blank M, Sims NA. Cellular processes by which osteoblasts and osteocytes control bone mineral deposition and maturation revealed by stage-specific EphrinB2 knockdown. *Curr Osteoporos Rep.* 2019;17(5):270-280.
21. Kolb PS, Ayaub EA, Zhou W, Yum V, Dickhout JG, Ask K. The therapeutic effects of 4-phenylbutyric acid in maintaining proteostasis. *Int J Biochem Cell Biol.* 2015;61:45-52.
22. Besio R, Iula G, Garibaldi N, et al. 4-PBA ameliorates cellular homeostasis in fibroblasts from osteogenesis imperfecta patients by enhancing autophagy and stimulating protein secretion. *Biochim Biophys Acta Mol Basis Dis.* 2018;1864(5 Pt A):1642-1652.
23. Besio R, Garibaldi N, Leoni L, et al. Cellular stress due to impairment of collagen prolyl hydroxylation complex is rescued by the chaperone 4-phenylbutyrate. *Dis Model Mech.* 2019;12(6):dmm038521.
24. Gioia R, Tonelli F, Ceppi I, et al. The chaperone activity of 4PBA ameliorates the skeletal phenotype of Chihuahua, a zebrafish model for dominant osteogenesis imperfecta. *Hum Mol Genet.* 2017;26(15):2897-2911.
25. Duran I, Zieba J, Csukasi F, et al. 4-PBA treatment improves bone phenotypes in the Aga2 mouse model of osteogenesis imperfecta. *J Bone Miner Res.* 2022;37(4):675-686.
26. Scheiber AL, Guess AJ, Kaito T, et al. Endoplasmic reticulum stress is induced in growth plate hypertrophic chondrocytes in G610C mouse model of osteogenesis imperfecta. *Biochem Biophys Res Commun.* 2019;509(1):235-240.
27. Scheiber AL, Wilkinson KJ, Suzuki A, et al. 4PBA reduces growth deficiency in osteogenesis imperfecta by enhancing transition of hypertrophic chondrocytes to osteoblasts. *JCI Insight.* 2022;7(3):e149636.
28. Rocha S, Ferraz R, Prudêncio C, Fernandes MH, Costa-Rodrigues J. Differential effects of antiepileptic drugs on human bone cells. *J Cell Physiol.* 2019;234(11):19691-19701.
29. Misra A, Aggarwal A, Singh O, Sharma S. Effect of carbamazepine therapy on vitamin D and parathormone in epileptic children. *Pediatr Neurol.* 2010;43(5):320-324.
30. Kumandas S, Koklu E, Gümüş H, et al. Effect of carbamazepine and valproic acid on bone mineral density, IGF-I and IGFBP-3. *J Pediatr Endocrinol Metab.* 2006;19(4):529-534.
31. Hoikka V, Alhava EM, Karjalainen P, et al. Carbamazepine and bone mineral metabolism. *Acta Neurol Scand.* 1984;70(2):77-80.
32. Vestergaard P, Rejnmark L, Mosekilde L. Fracture risk associated with use of antiepileptic drugs. *Epilepsia.* 2004;45(11):1330-1337.
33. Kim SH, Lee JW, Choi KG, Chung HW, Lee HW. A 6-month longitudinal study of bone mineral density with antiepileptic drug monotherapy. *Epilepsy Behav.* 2007;10(2):291-295.
34. Sheth RD, Wesolowski CA, Jacob JC, et al. Effect of carbamazepine and valproate on bone mineral density. *J Pediatr.* 1995;127(2):256-262.
35. Ecevit C, Aydoğan A, Kavaklı T, Altinöz S. Effect of carbamazepine and valproate on bone mineral density. *Pediatr Neurol.* 2004;31(4):279-282.
36. Erbayat Altay E, Serdaroğlu A, Tümer L, Gücüyener K, Hasanoğlu A. Evaluation of bone mineral metabolism in children receiving carbamazepine and valproic acid. *J Pediatr Endocrinol Metab.* 2000;13(7):933-939.
37. Akin R, Okutan V, Sarici U, Altunbas A, Gökçay E. Evaluation of bone mineral density in children receiving antiepileptic drugs. *Pediatr Neurol.* 1998;19(2):129-131.
38. Diemar SS, Sejling AS, Eiken P, et al. Effects of carbamazepine, eslicarbazepine, valproic acid and levetiracetam on bone microarchitecture in rats. *Pharmacol Rep.* 2020;72(5):1323-1333.
39. Parveen B, Tiwari AK, Jain M, et al. The anti-epileptic drugs valproate, carbamazepine and levetiracetam cause bone loss and modulate Wnt inhibitors in normal and ovariectomised rats. *Bone.* 2018;113:57-67.
40. Enlow DH. A study of the post-natal growth and remodeling of bone. *Am J Anat.* 1962;110:79-101.
41. Isojima T, Sims NA. Cortical bone development, maintenance and porosity: genetic alterations in humans and mice influencing chondrocytes, osteoclasts, osteoblasts and osteocytes. *Cell Mol Life Sci.* 2021;78(15):5755-5773.

SUPPORTING INFORMATION

Additional supporting information may be found in the online version of the article at the publisher's website.

How to cite this article: Blank M, McGregor NE, Rowley L, et al. The effect of carbamazepine on bone structure and strength in control and osteogenesis imperfecta (*Col1a2*^{+/*p.G610C*}) mice. *J Cell Mol Med.* 2022;26:4021-4031. doi: [10.1111/jcmm.17437](https://doi.org/10.1111/jcmm.17437)